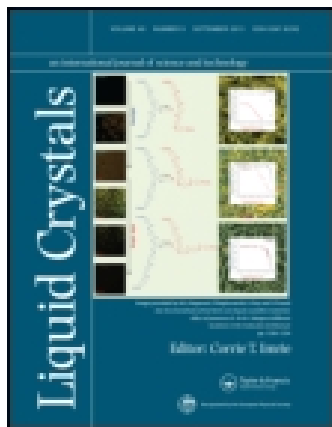


This article was downloaded by: [Shanghai Jiaotong University]

On: 24 October 2014, At: 18:26

Publisher: Taylor & Francis

Informa Ltd Registered in England and Wales Registered Number: 1072954 Registered office: Mortimer House, 37-41 Mortimer Street, London W1T 3JH, UK



## Liquid Crystals

Publication details, including instructions for authors and subscription information:

<http://www.tandfonline.com/loi/tlct20>

### The Influence of polymer system on polymer-stabilised blue phase liquid crystals

Ji-Liang Zhu<sup>a</sup>, Shui-Bin Ni<sup>a</sup>, Chao Ping Chen<sup>a</sup>, Xiao-Long Song<sup>b</sup>, Chao-Yuan Chen<sup>b</sup>, Jian-Gang Lu<sup>a</sup> & Yikai Su<sup>a</sup>

<sup>a</sup> National Engineering Laboratory of TFT-LCD Materials and Technologies, Department of Electronic Engineering, Shanghai Jiao Tong University, Shanghai, China

<sup>b</sup> The research and development center of flat-display materials engineering technology, The Jiangsu Hecheng Display Technology Co., Ltd, Nanjing, China

Published online: 23 Jan 2014.



[Click for updates](#)

To cite this article: Ji-Liang Zhu, Shui-Bin Ni, Chao Ping Chen, Xiao-Long Song, Chao-Yuan Chen, Jian-Gang Lu & Yikai Su (2014) The Influence of polymer system on polymer-stabilised blue phase liquid crystals, *Liquid Crystals*, 41:6, 891-896, DOI: [10.1080/02678292.2014.882023](https://doi.org/10.1080/02678292.2014.882023)

To link to this article: <http://dx.doi.org/10.1080/02678292.2014.882023>

PLEASE SCROLL DOWN FOR ARTICLE

Taylor & Francis makes every effort to ensure the accuracy of all the information (the "Content") contained in the publications on our platform. However, Taylor & Francis, our agents, and our licensors make no representations or warranties whatsoever as to the accuracy, completeness, or suitability for any purpose of the Content. Any opinions and views expressed in this publication are the opinions and views of the authors, and are not the views of or endorsed by Taylor & Francis. The accuracy of the Content should not be relied upon and should be independently verified with primary sources of information. Taylor and Francis shall not be liable for any losses, actions, claims, proceedings, demands, costs, expenses, damages, and other liabilities whatsoever or howsoever caused arising directly or indirectly in connection with, in relation to or arising out of the use of the Content.

This article may be used for research, teaching, and private study purposes. Any substantial or systematic reproduction, redistribution, reselling, loan, sub-licensing, systematic supply, or distribution in any form to anyone is expressly forbidden. Terms & Conditions of access and use can be found at <http://www.tandfonline.com/page/terms-and-conditions>

## The Influence of polymer system on polymer-stabilised blue phase liquid crystals

Ji-Liang Zhu<sup>a</sup>, Shui-Bin Ni<sup>a</sup>, Chao Ping Chen<sup>a</sup>, Xiao-Long Song<sup>b</sup>, Chao-Yuan Chen<sup>b</sup>, Jian-Gang Lu<sup>a\*</sup> and Yikai Su<sup>a</sup>

<sup>a</sup>National Engineering Laboratory of TFT-LCD Materials and Technologies, Department of Electronic Engineering, Shanghai Jiao Tong University, Shanghai, China; <sup>b</sup>The research and development center of flat-display materials engineering technology, The Jiangsu Hecheng Display Technology Co., Ltd, Nanjing, China

(Received 18 September 2013; accepted 7 January 2014)

The influence of polymer system on polymer-stabilised (PS) blue phase (BP) liquid crystal (LC) is investigated. After polymer stabilisation, anchoring energy appears between the polymer network and LC molecules, which is related with the stiffness of the polymer system. As the stiffness of polymer system decreases, the Kerr constant can be improved with the degradation of response time, hysteresis, and residual birefringence. Furthermore, the Kerr constant and response time can be improved simultaneously by polymer system with reactive diluents.

**Keywords:** blue phase; polymer system; Kerr constant; polymer-stabilised; hysteresis

### 1. Introduction

Blue phase (BP) liquid crystals (LCs) appear as a regular array of double twist cylinders (DTCs) separated by a network of disclination lines in a narrow temperature range between the isotropic phase and the chiral nematic (N\*) phase.[1–4] Recently, the temperature range of BPLCs, usually less than several Kelvins, has been broadened to more than 60 K by stabilising the disclination cores with amorphous polymer chains localised within them.[5] Polymer-stabilised (PS) BPLCs promise great potential applications in field sequential displays,[6,7] phase modulator devices,[8–10] and three-dimensional (3-D) tunable photonic crystals [11,12] owing to their interesting features, including sub-millisecond response time, optical isotropic status in the absence of electric field, and 3-D helical structure with a periodicity on the order of the visible wavelength. However, there are still several issues to be overcome before wide applications of the PS-BPLCs, such as high driving voltage, hysteresis, and residual birefringence. [13–15] To improve the electro-optic performance of the PS-BPLCs, several studies have been carried out, such as the effects of chiral pitch,[16] polymerisation process,[17,18] and polymer concentration on BPLCs. [19,20] Nevertheless, the anchoring energy of the polymer network system which may have significant effect on the properties of the PS-BPLCs has rarely been studied.

In this paper, the effects of polymer system on the thermal stability and electro-optic properties of PS-BPLCs are investigated. As the stiffness of polymer system increases, the anchoring energy of polymer system increases, resulting in the decrease of Kerr

constant, hysteresis, response time, and residual birefringence. Nevertheless, by a polymer system with reactive diluents, the Kerr constant and response time can be improved simultaneously. The residual birefringence can be removed by thermal energy since the deformation of PS-BPLC lattice structure induced by applied electric field can be recovered by the thermal energy.

### 2. Materials and experiments

To investigate the effect of polymer system on the PS-BPLC, several kinds of the monomers were doped in the mixture of conventional materials to stabilise the disclination lines in the BPLCs. Here, the conventional PS-BPLC mixture was chosen to be composed of a positive nematic liquid crystal (BP-06,  $\Delta n = 0.158$ ,  $\Delta\epsilon = 34.2$ , Jiangsu Hecheng Display Technology Co., Ltd. (HCCH)), a chiral dopant (R5011, HCCH), a cross-linking agent (RM257), an ultraviolet (UV) curable monomer (TMPTA 1,1,1-Trimethylolpropane Triacrylate, HCCH), and a photoinitiator (IRG184, HCCH). As the number of functional group increases and the chain length of monomer decreases, the stiffness of polymer system increases, resulting in a larger anchoring energy of the polymer network. To make the polymer system with different anchoring energy, a cross-linking agent, RM257, and four kinds of monomers with different chemical structures, TMPTA, NVP (N-vinylpyrrolidone), ACOMO (Acryloyl morpholine), and 12A, were chosen in this experiment. The chemical structures of the monomers are illustrated in Table 1. Among them, RM257 is a di-function monomer,

\*Corresponding author. Email: [lujg@sjtu.edu.cn](mailto:lujg@sjtu.edu.cn)

Table 1. The chemical structure of monomers.

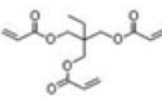
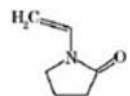
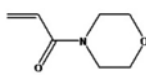
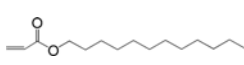
Type	Name	Chemical structure	
Tri-function monomer	TMPTA		Three-dimensional
Mono-function monomer	NVP		Five-membered ring
	ACMO		Six-membered ring
	12A		Linearity

Table 2. Summary of PS-BPLC precursors with different component ratios.

Precursors	BPLC (%)	RM257 (%)	TMPTA (%)	Monomers	IRG184 (%)
A	89.5	4.4	5.5		0.6
B	89.5	3.3	3.3	3.3% (NVP)	0.6
C	89.5	3.3	3.3	3.3% (ACMO)	0.6
D	89.5	3.3	3.3	3.3% (12A)	0.6

TMPTA is a tri-function monomer, and NVP, ACMO, and 12A are mono-function monomers.

For comparison, precursors were prepared in the same condition, as listed in Table 2. The chiral pitches were controlled at about 329 nm by adjusting the chiral concentration because the electric-optic performance of PS-BPLCs is related with their chiral pitch. [21,22] To keep the total concentration of monomers from affecting the properties of PS-BPLC, the overall monomers concentration in the precursors was fixed at 9.9% by weight. After homogeneous mixing, the precursors were filled into in-plane switching (IPS) cells, whose cell gap is 7.5  $\mu\text{m}$ , the indium tin oxide (ITO) electrode width is 7.5  $\mu\text{m}$  and the electrode gap is 12.5  $\mu\text{m}$ , at the isotropic phase in a temperature controller (HCS302, Instec Co., USA). To measure the electro-optic properties of the PS-BPLC, a white light-emitting diode (LED) was used as a light source to avoid the diffraction of the IPS devices. [9,10,23] The IPS cells applied with a 1 kHz square-wave AC signal was placed between two crossed polarisers. The

transmittance was detected with a spectrometer (HR4000, Ocean optic Co., USA). The PS-BPLC reflects light in green regime owing to their Bragg reflection. To avoid the Bragg reflection, one can either change the pitch of PS-BPLC, or shift the reference wavelength. Here, the reference wavelength of our IPS devices was set to 633 nm.

### 3. Results and discussion

#### 3.1. Thermal stability

To study the influence of polymer system on the thermal stability, the samples were irradiated at blue phase, whose chiral pitch was about 329 nm, under an ultraviolet light with an intensity of 3  $\text{mW} \cdot \text{cm}^{-2}$ . After 15 minutes exposure, the clearing point of the samples A, B, C, and D was 338 K. The phase transition of the samples was observed under a reflective polarising optical microscopy during the cooling process (338–263 K). The cooling rate was 0.2  $\text{K} \cdot \text{min}^{-1}$  and is controlled by the temperature controller (HCS302, Instec Co.). The blue phases of the samples A, B, C, and D were observed when the temperature was cooled down to 263 K. Figure 1(a), (c), (e), and (g) shows the platelet textures of the samples when the temperature was cooled down to 313 K. As the temperature was further cooled, the blue phase was observed in samples A, B, C, and D at 265 K (Figure 1(b), (d), (f), and (h)). The blue phase temperature ranges of samples A, B, C, and D were all expanded to more than 70 K (263–338 K) after polymerisation.

#### 3.2. Kerr constant

The voltage-dependent transmittance (V-T) curves of the IPS devices were measured by applying a square wave voltage with 1-kHz frequency. Figure 2 shows the normalised V-T curves of our devices. At the room temperature ( $\sim 299$  K), the on-state voltages ( $V_{\text{on}}$ ) of samples A, B, C, and D are 145, 118, 105, and 90 V, respectively. Among the samples, sample A has the highest  $V_{\text{on}}$  and sample D has the lowest  $V_{\text{on}}$ . As shown in Figure 2, there is a mismatch between the normalised V-T curves of sample D before ultraviolet irradiation and after ultraviolet irradiation, which is attributed to the anchoring energy between the polymer system and DTCs.

According to the extended Kerr effect, [24] the induced birefringence ( $\Delta n_{\text{ind}}$ ) of PS-BPLCs is related to the electric field.

$$\Delta n_{\text{ind}} = \Delta n_s (1 - \exp[-(E/E_s)^2]) \quad (1)$$

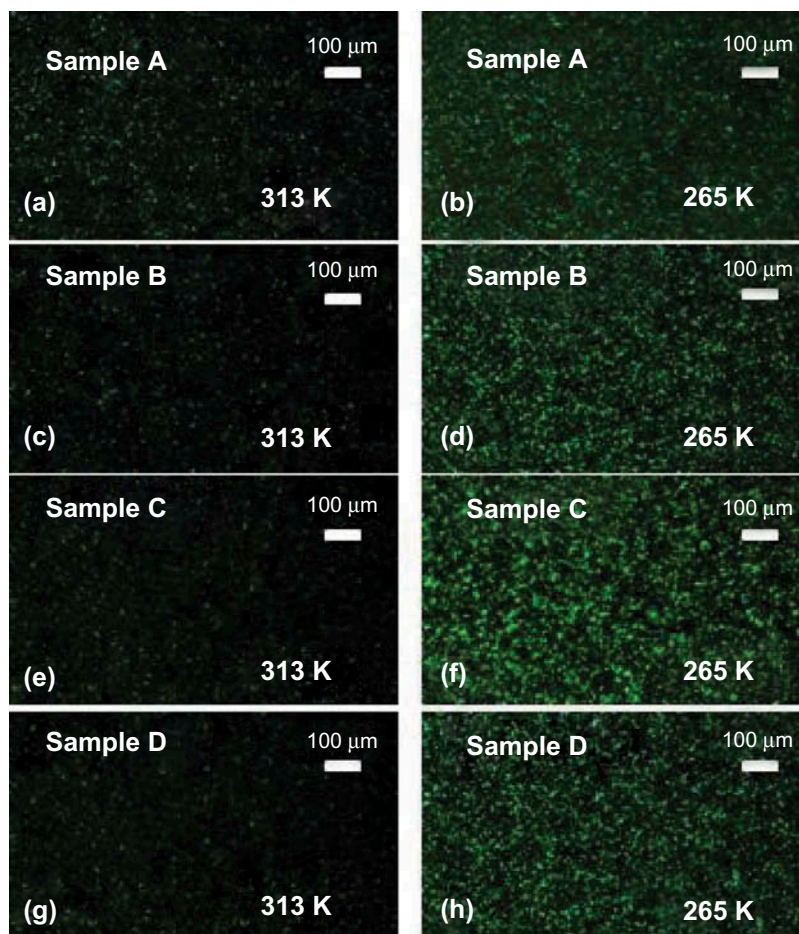


Figure 1. (colour online) Platelet textures of the PS-BPLC samples under a polarised optical microscope (POM).

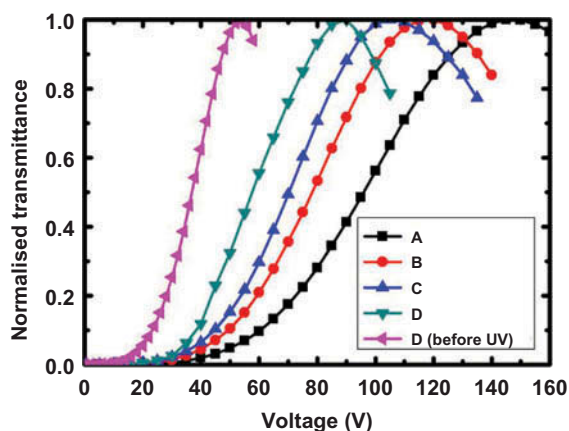


Figure 2. (colour online) Normalised voltage-dependent transmittance (V-T) curves of the samples at 299 K,  $\lambda = 633$  nm.

where  $\Delta n_s$  is the saturated induced birefringence and  $E_s$  is the saturation electric field. In the weak field region, the Kerr constant is derived as follows:

$$K \approx \Delta n_s / (\lambda E_s^2) \quad (2)$$

The Kerr constant is obtained by fitting the V-T curves with the extended Kerr effect model. The electric field of our IPS devices was simulated with software TechWiz LCD 3D (Sanayi System, Taiwan). The Kerr constants of sample A, B, C, and D are  $1.5 \text{ nmV}^{-2}$ ,  $2.3$ ,  $2.9$ , and  $3.9 \text{ nmV}^{-2}$ , respectively. Among the samples, the Kerr constant of sample A is the smallest one since the anchoring energy of polymer system formed by RM 257 and TMPTA, a tri-function monomer, is higher than that of the other polymer system formed with a mono-function monomer or a di-function monomer. Although the NVP and ACMO show the similar chemical structure, the Kerr constant of sample B is smaller than that of sample C because the anchoring energy of polymer formed with a five-membered ring is higher than that formed with a six-membered ring with oxygen. Compared to the sample A, B, and C, sample D shows a smaller Kerr constant owing to its low

anchoring energy originating from the polymer system with flexible linear side chains.

### 3.3. Hysteresis

Hysteresis is a key issue that affects the grayscale in LC displays and it should be solved before the wide application of PS-BPLCs. To measure the hysteresis of our IPS devices, the IPS devices were driven by switching the applied voltage upwards to  $V_{on}$  and then downwards to zero, as shown in Figure 3(a). The hysteresis is defined as  $\Delta V/V_{on}$ , where  $\Delta V$  is the voltage difference between the upward and downward scans at half of the peak transmittance. According to the measured V-T curves, the hysteresis of samples are 2.4%, 4.8%, 5.6%, and 6.2% at their  $V_{on}$ , respectively, as shown in Table 3. Among the samples, the hysteresis of sample A is the lowest one and that of sample D is the largest one. The hysteresis of sample B is larger than that of sample C. Figure 3(b) shows the hysteresis of sample B with different applied

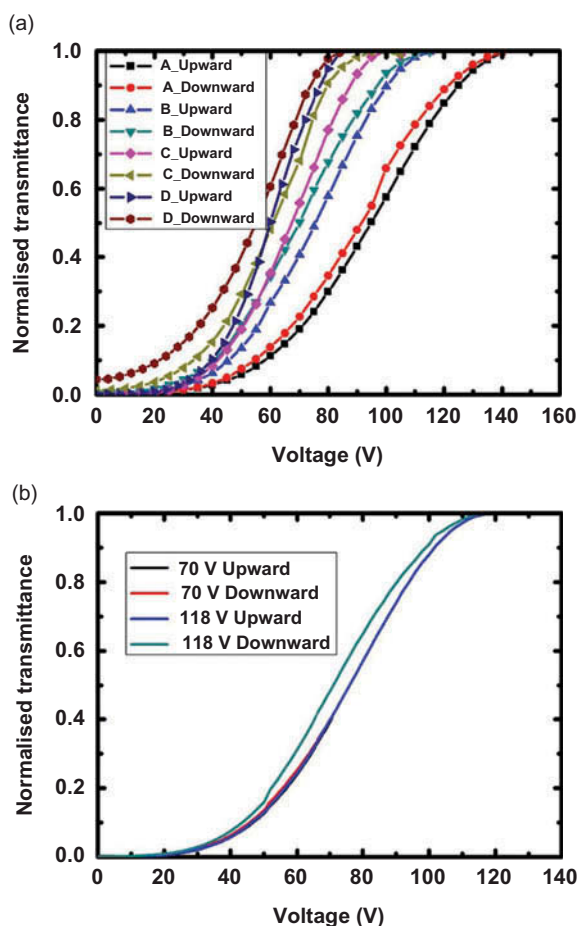


Figure 3. (colour online) (a) Measured normalised V-T curves for hysteresis of the samples; (b) the hysteresis of sample B with different applied voltages,  $\lambda = 633$  nm.

Table 3. The hysteresis, residual birefringence, and decay time of samples.

Samples	A	B	C	D
Hysteresis (%)	2.4	4.8	5.6	6.2
Residual birefringence (%)	0.22	0.35	1.14	4.35
Decay time ( $\mu$ s)	575	523	934	1240

voltages. The V-T curves of the sample B were fitted well when the device was driven by switching the applied voltage upwards to 70 V and then downwards to zero, resulting in free-hysteresis. An obvious hysteresis is observed in sample B at its  $V_{on}$ . Therefore, there is a critical electric field ( $E_c$ ) for hysteresis of PS-BPLCs. If the applied electric field is less than  $E_c$ , the hysteresis-free can be achieved.

Figure 4 shows the schematic diagram of polymer chain surrounded by liquid crystal molecules. The alignment of the liquid crystal molecules is related to the polymer chains due to the anchoring energy between polymer chains and liquid crystal molecules. Macroscopically, a PS-BPLC is considered as an optically isotropic material without electric field (Figure 4(a)). After the electric field was applied, the BPLC molecules and the polymer chain are induced to dipole movement (Figure 4(b)). As shown in Figure 3(b), if the applied electric field is less than  $E_c$ , the PS-BPLC shows hysteresis-free since the BPLC molecules and polymer chain recover automatically to their original state (Figure 4(a)). Otherwise, if the applied electric field exceeds  $E_c$ , the hysteresis will appear because the BPLC molecules and the deformed polymer chain (Figure 4(c)) cannot fully relax to its original state. As the stiffness of polymer system increases, the hysteresis of PS-BPLC device can be suppressed since the distorted polymer system with higher stiffness is conducive to be recovered. The hysteresis of sample A is lower

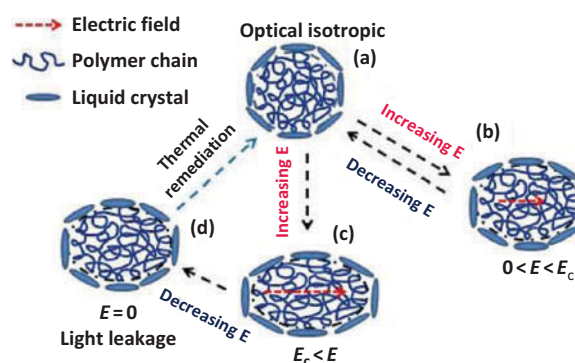


Figure 4. (colour online) Schematic diagram of the polymer network surrounded by liquid crystals with different electric field.

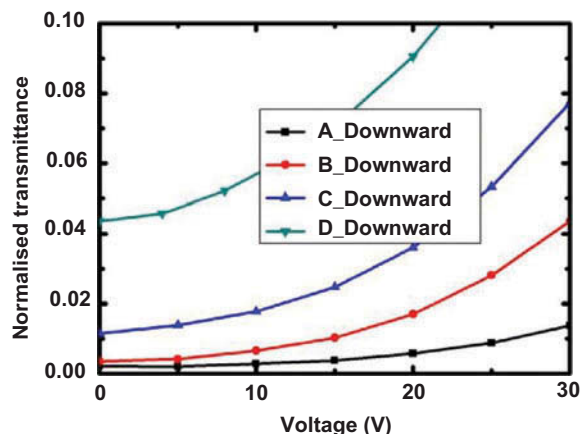


Figure 5. (colour online) The residual birefringence of the samples at 299 K,  $\lambda = 633$  nm.

than that of the other samples owing to the highest stiffness of polymer system formed with TMPTA. Compared to the other samples, the hysteresis of sample D is larger one because of its lower stiffness of the polymer system formed with a high flexible linear side chains. The hysteresis of sample B is lower than that of sample C because the stiffness of polymer formed with a five-membered ring is larger than that formed with a six-membered ring with oxygen.

### 3.4. Residual birefringence

Residual birefringence is another key issue which should be solved before the wide application of PS-BPLCs. Here, the residual birefringence is defined as  $T_0$ , where  $T_0$  is the normalised transmittance at  $V = 0$  V during the voltage downward process, as shown in Figure 5. According to the measured V-T curves, the residual birefringence of samples are 0.22%, 0.35%, 1.14%, and 4.35%, respectively, as shown in Table 3. Similar to the hysteresis, sample A shows the lowest residual birefringence and sample D shows the largest residual birefringence. The residual birefringence of sample C is larger than that of sample B.

The distortion will happen if the applied electric field exceeds  $E_c$ . Therefore, after the applied electric field was removed, the LC molecules around polymer chain cannot recover to its original state due to the distorted polymer chain and the anchoring energy between polymer chains and the LC molecules, resulting in residual birefringence, as shown in Figure 4(d). As the stiffness of polymer system increases, the residual birefringence of PS-BPLC will decrease because the deformed structure of polymer chain is easier to recover to its original state. The devices were heated in a temperature controller. When the temperature of

the PS-BPLC is close to its clearing point, the residual birefringence of the device disappeared because the deformed structure (Figure 4(c)) of polymer chain is recovered to its original state (Figure 4(a)) by the thermal energy.

### 3.5. Response time

For PS-BPLCs, the fast response time is one of the major attractions. As the rise time depends on the driving voltage, we only evaluate the decay time in this paper. As listed in Table 3, the decay time of sample D is the slowest one among the samples because anchoring energy of sample D is the lowest one due to its polymer system with a high flexible linear side chains. The decay time of sample A is faster than that of sample C because the anchoring energy of polymer system formed with RM 257 and TMPTA, a tri-function monomer, is higher than that of polymer system formed by RM257 and ACMO, a mono-function monomer. Anyhow, the decay time will decrease as the anchoring energy of polymer system increases.

### 3.6. Discussion

Comparing the sample D with the sample A, the Kerr constant can be increased by 160% and the decay time will be increased by 110%. If the applied electric field is less than  $E_c$ , the PS-BPLC device will be hysteresis-free. Though the anchoring energy of sample A is larger than that of sample B, the decay time of sample B is faster than that of sample A. A reactive diluent can be formed by NVP and acrylic functional groups of the RM257 and TMPTA after polymerisation and can decrease the effective rotational viscosity of the material system, resulting in a fast response time. According to aforementioned, the Kerr constant of sample B is larger than that of sample A. Anyhow, by using the polymer system with reactive diluents and limiting the applied electric to  $E_c$ , a novel PS-BPLC device with large Kerr constant, fast response time, and hysteresis-free will be obtained.

## 4. Conclusions

The effects of polymer system on the thermal stability and electro-optic properties of PS-BPLC are investigated. The experimental results indicate that the electro-optic properties of PS-BPLC are affected by anchoring energy of polymer system. As the anchoring energy of polymer system decreases, the Kerr constant increases with the degradation of response time, hysteresis and residual birefringence. However, the Kerr constant and response time can

be improved simultaneously by polymer system with reactive diluents.

### Funding

This work was sponsored by 973 Program [grant number 2013CB328804]; NSFC [grant number 61275026].

### References

- [1] Kitzerow HS, Crooker PP, Kwok SL, Xu J, Heppke G. Dynamics of blue-phase selective reflections in an electric field. *Phys Rev A*. 1990;42:3442–3448.
- [2] Haseba Y, Kikuchi H. Optically isotropic chiral liquid crystals induced by polymer network and their electro-optical behavior. *Mol Cryst Liq Cryst*. 2007;470(1):1–9.
- [3] Meiboom S, Sethna JP, Anderson PW, Brinkman WF. Theory of the blue phase cholesteric liquid crystals. *Phys Rev L*. 1981;46(18):1216–1219.
- [4] Zheng ZG, Shen D, Huang P. Wide blue phase range of chiral nematic liquid crystal doped with bent-shaped molecules. *New J Phys*. 2010;12:113018(10).
- [5] Kikuchi H, Yokota M, Hisakado Y, Yang H, Kajiyama T. Polymer-stabilized liquid crystal blue phases. *Nat Mater*. 2002;1(1):64–68.
- [6] Chen KM, Gauza S, Xianyu HQ, Wu ST. Hysteresis effects in blue-phase liquid crystals. *J Disp Technol*. 2010;6(8):318–322.
- [7] Kim M, Kang BG, Kim MS, Kim MK, Kumar P, Lee MH, Kang SW, Lee SH. Measurement of local retardation in optically isotropic liquid crystal devices driven by in-plane electric field. *Curr Appl Phys*. 2010;10:e118–e121.
- [8] Lu SY, Chien LC. Electrically switched color with polymer-stabilized blue-phase liquid crystals. *Opt Lett*. 2010;35:562–564.
- [9] Yan J, Li Y, Wu ST. High-efficiency and fast-response tunable phase grating using a blue phase liquid crystal. *Opt Lett*. 2011;36(8):1404–1406.
- [10] Zhu G, Li JN, Lin XW, Wang HF, Hu W, Zheng ZG, Cui HQ, Shen D, Lu YQ. Polarization-independent blue-phase liquid-crystal grating driven by vertical electric field. *J Soc Inf Disp*. 2012;20(6):341–346.
- [11] Coles H, Morris S. Liquid-crystal lasers. *Nature Photonics*. 2010;4(10):676–685.
- [12] Yokoyama S, Mashiko S, Kikuchi H, Uchida K, Nagamura T. Laser emission from a polymer-stabilized liquid-crystalline blue phase. *Adv Mater*. 2006;18:48–51.
- [13] Choi H, Higuchi H, Kikuchi H. Fast electro-optic switching in liquid crystal blue phase II. *Appl Phys Lett*. 2011;98:131905.
- [14] Lin YH, Chen HS, Lin HC, Tson YS, Hsu HK, Li WY. Polarizer-free and fast response microlens arrays using polymer-stabilized blue phase liquid crystals. *Appl Phys Lett*. 2010;96:113505.
- [15] Wang L, He WL, Xiao X, Meng FG, Zhang Y, Yang PY, Wang LP, Xiao JM, Yang H, Lu YF. Hysteresis-free blue phase liquid-crystal-stabilized by ZnS nanoparticles. *Small*. 2012;8:2189–2193.
- [16] Choi H, Higuchi H, Higuchi H. Electrooptic response of liquid crystalline blue phases with different chiral pitches. *Soft Matter*. 2011;7:4252–4256.
- [17] Zhu JL, Ni SB, Zhong EW, Lu JG, Su YK. Polymerization effect on blue phase liquid crystals. Paper presented at: SID Display Week 2012; 2012 June 3–8; Boston Massachusetts, USA.
- [18] Fan CY, Jau HC, Lin TH, Yu FC, Huang TH, Liu C, Sugiura N. Influence of polymerization temperature on hysteresis and residual birefringence of polymer stabilized blue phase LC. *J Disp Technol*. 2011;7:615–618.
- [19] Yan J, Wu ST. Effect of polymer concentration and composition on blue-phase liquid crystals. *J Disp Technol*. 2011;7(9):490–493.
- [20] Oo TN, Mizunuma T, Nagano Y, Ma H, Ogawa Y, Haseba Y, Higuchi H, Okumura Y, Kikuchi H. Effects of monomer/liquid crystal compositions on electro-optical properties of polymer-stabilized blue phase liquid crystal. *Opt Mater Express*. 2011;1:1502–1510.
- [21] Rao LH, Yan J, Wu ST, Yamamoto S, Haseba Y. A large Kerr constant polymer-stabilized blue phase liquid crystal. *Appl Phys Lett*. 2011;98:081109.
- [22] Gerber R. Electro-optical effects of a small-pitch blue-phase system. *Mol Cryst Liq Cryst*. 1985;116:197–206.
- [23] Zhu JL, Lu JG, Qiang J, Zhong EW, Ye ZC, He ZH, Guo XJ, Dong CY, Su YK, Shieh HP. 1D/2D switchable grating based on field-induced polymer stabilized blue phase liquid crystal. *J Appl Phys*. 2012;111:033101.
- [24] Yan J, Cheng HC, Gauza S, Li Y, Jiao MZ, Rao LG, Wu ST. Extended Kerr effect of polymer-stabilized blue-phase liquid crystals. *Appl Phys Lett*. 2010;96:071105.